Available online at www.sciencedirect.com

ScienceDirect

Proceedings of the Combustion Institute 39 (2023) 551–560

Proceedings of the Combustion Institute

www.elsevier.com/locate/proci

On the role of HNNO in NO_x formation

Qinghui Meng [a], Lei Lei [a], Joe Lee [a], Michael P. Burke [a,b,*]

[a] *Dept. of Mech. Eng., Columbia University, New York, NY, USA*
[b] *Dept. of Chem. Eng. and Data Sciences Institute, Columbia University, New York, NY, USA*

Received 6 January 2022; accepted 17 August 2022
Available online 19 January 2023

Abstract

The formation of nitrogen oxides (NO_x) during combustion is a topic of substantial fundamental and practical interest, given the complex nature of its formation kinetics and the fact that, as a highly regulated pollutant emission, it is a major constraint in engineering design. To date, there are four known mechanisms by which the strong N–N bond can be broken to facilitate NO_x formation from N_2 present in air. Here we posit and explore the possibility of a new NO_x formation route mediated by an HNNO intermediate whose reactions with common combustion species break the N–N bond. Altogether, we present results from master equation (ME) calculations for HNNO formation from H + N_2O (+M), ab initio electronic structure and RRKM/ME calculations for HNNO + O_2, and simulations of NO profiles in freely propagating flames using a newly constructed HNNO kinetic sub-model. Our ME results for the H + N_2O reaction indicate that HNNO is the favored product channel at lower temperatures and higher pressures – e.g. favored over all other products up to ∼1100 K and over NH + NO up to ∼1500 K above 10 atm. Our ab initio electronic structure calculations for trans-HNNO + O_2 show a barrier for abstraction to HO_2 + N_2O of 18.2 kcal/mol and a barrier for addition of 27.0 kcal/mol to form an HN(OO)NO which can decompose to NO + HNO_2 over a barrier of 32.3 kcal/mol (cis-HNNO + O_2 shows similar reactivity). Altogether, our rate constant calculations and kinetic modeling, which also includes estimated rate constants for HNNO + radical reactions, suggest that HNNO + O_2 mainly recycles HNNO back to N_2O but is sufficiently slow that the primary fate of HNNO in many combustion situations likely involves reactions with radical species, which appear likely to occur quickly and with high NO_x yields.

Keywords: Flame chemistry; Pollutant emissions; Ab initio theoretical calculations; Kinetic modeling; Nitrogen chemistry

1. Introduction

Nitrogen oxides (NO_x), which lead to ground-level ozone and smog detrimental to human and environmental health, are undesirable by-products of combustion. It has long been known that NO_x is formed not only for nitrogenous fuels but also from

* Corresponding author.
E-mail address: mpburke@columbia.edu (M.P. Burke).

https://doi.org/10.1016/j.proci.2022.08.044

nonnitrogenous fuels when burned in air [1,2]. In the latter case, NO_x is formed from N_2 in air during combustion, which requires breaking the strong N–N bond in N_2. These mechanisms are both kinetically limited under many conditions and extraordinarily complex. NO_x can be formed from multiple different pathways, each of which are exquisitely – and uniquely – sensitive to temperature, pressure, and mixture composition. Consequently, NO_x formation rates vary significantly with thermodynamic conditions. On one hand, this has of course offered significant opportunities for their mitigation, which is often a major constraint in engineering design. On the other hand, its inherent complexity complicates the design of the most advanced low-NO_x engines, where multiple pathways often contribute substantively to NO_x formation [3].

Perhaps the most daunting feature of its kinetics is that the dominant pathways themselves also vary significantly with thermodynamic conditions. Therefore, even if the magnitude of NO_x can be quantitatively predicted at specific laboratory or engine configurations, extrapolating to new situations [4] and/or identifying the best design configuration [3] are both presently elusive goals.

Central to both of those scientific and engineering objectives is knowledge of the NO_x formation routes from N_2 during combustion. To date, there are four known mechanisms by which the N–N bond can be broken to facilitate NO_x formation [2].

In the Zeldovich mechanism [5], the N–N bond is broken via reaction of atmospheric N_2 with O

$$O + N_2 \longleftrightarrow NO + N \quad (1)$$

yielding NO_x directly and indirectly via reaction of the co-product N with O_2 or OH.

In the Fenimore mechanism [6], the N–N bond is usually broken via reaction of atmospheric N_2 with CH in a reaction that is now known [7] to be:

$$CH + N_2 \longleftrightarrow NCN + H \quad (2)$$

where NO_x is indirectly formed via subsequent reactions initiated by NCN.

In the NNH mechanism [8], the N–N bond is broken via reaction of an NNH intermediate, produced by

$$H + N_2(+M) \longleftrightarrow NNH(+M) \quad (3)$$

with O:

$$NNH + O \longleftrightarrow NO + NH \quad (4)$$

where the NH co-product yields additional NO_x production.

In the N_2O mechanism [9], the N–N bond is broken via reactions of an N_2O intermediate, produced by

$$O + N_2(+M) \longleftrightarrow N_2O(+M) \quad (5)$$

with O and H

$$N_2O + O \longleftrightarrow NO + NO \quad (6)$$

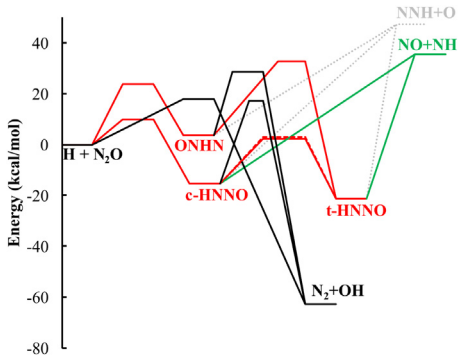

Fig. 1. Potential energy surface (PES) [13] for H + N_2O.

$$N_2O + H \longleftrightarrow NO + NH \quad (7)$$

where similarly the NH co-product yields additional NO_x production. Of note, the N_2O route is often the dominant NO_x formation pathway at the high-pressure, low-temperature conditions of high-efficiency, low-NO_x engines [3,10,11], where low temperatures reduce Zeldovich NO_x [10] and high pressures reduce Fenimore NO_x [3,12] and increase N_2O formation [3]. NO_x formation through the N_2O route crucially depends on the fate of N_2O. The reaction of N_2O with H is generally considered to predominantly form N_2 + OH with only a minor yield to NH + NO. The H + N_2O branching ratio among products is therefore known to be a key factor in high-pressure NO formation.

However, the H + N_2O reaction can proceed via HNNO* complexes which can decompose to either of the two main bimolecular product channels, N_2 + OH or NH + NO [13,14] (Fig. 1). Interestingly, theoretical calculations show significant HNNO stabilization at lower temperatures even at atmospheric pressure [13,14]. Given that relatively little of H + N_2O results in NO formation via NH + NO, even a small amount of HNNO stabilization, which would increase with pressure, could be significant. However, while some models include some HNNO chemistry, pressure dependence of H + N_2O – which would be essential to uncovering its role – is not generally included in kinetic models [13,15–19] and is not known to be important to NO_x formation.

Here we posit and present a first study of a new potential NO_x formation mechanism where the N–N bond is broken via reactions of HNNO. HNNO (which is used in this paper to collectively denote trans-HNNO, cis-HNNO, and ONHN) can be formed via the pressure-dependent reaction:

$$H + N_2O(+M) \longleftrightarrow HNNO(+M) \quad (8)$$

and, as discussed below, can participate in several possible reactions with common combustion species to yield NO_x. Based on the additional pressure-dependent stabilization process involved,

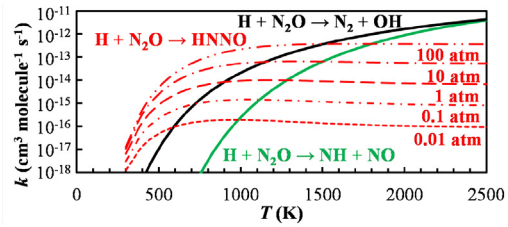

Fig. 2. Calculated rate constants for H + N_2O. (HNNO includes cis-HNNO, trans-HNNO, and ONHN.) Rate constants for H + N_2O → N_2 + OH and H + N_2O → NH + NO, which show little pressure dependence, are shown for low-pressure limit.

one might expect the HNNO route to become increasingly favored – over even the N_2O route – at higher pressures and lower temperatures.

We present results from master equation (ME) calculations for H + N_2O across a range of pressures using a published potential energy surface (PES) [13] which yield total H + N_2O rate constants at low temperatures, which are dominated by stabilization, consistent with atmospheric pressure experiments [20]. Indeed, as shown (cf. Fig. 2), our results show HNNO stabilization to be the preferred route at lower temperatures and higher pressures. In fact, above 10 atm, HNNO is the major product up to ~1100 K and is dominant over NH + NO up to ~1500 K.

Given that HNNO appears to be a major product from the H + N_2O reaction, its subsequent fate would be crucial to NO_x formation at high pressures. Limited rate constant data are available for reactions of HNNO, though theoretical studies of other reactions on the same PESs and our own preliminary ab initio studies suggest that H, OH, and O add to HNNO without an intrinsic energy barrier to form H_2NNO^*, $H_2NNO_2^*$, and $HNNO_2^*$ complexes [21–24]. In all cases, the features of the PES suggest roughly comparable decomposition to NO-forming and non-NO-forming routes.

Of course, HNNO could also react with O_2, which would be present in much higher fractions than radical species (especially for fuel-lean conditions). The rates and products from HNNO + O_2 are less clear but just as significant – if it were to occur quickly, it would likely be the dominant fate of HNNO and its branching ratio would dictate the role of HNNO in NO_x formation; if it were to occur slowly, the dominant fate of HNNO under many conditions would be reactions with radicals, which – as per above – are likely to occur quickly and with high NO_x yields.

Here we report results from an initial study that addresses two questions needed to determine the role of HNNO in NO_x formation: (1) under what conditions is HNNO production from H + N_2O significant? (2) what is the role of HNNO + O_2 in NO_x formation and HNNO consumption? To this end, we present results from ME calculations for H + N_2O, ab initio electronic structure theory and RRKM/ME calculations for HNNO + O_2, and simulations of premixed freely propagating flames using a new kinetic sub-model that includes our calculated rate constants for H + N_2O and HNNO + O_2 and calculated and/or estimated rate constants and branching ratios for HNNO + radical reactions.

2. Theoretical and numerical methods

The role of HNNO in NO_x formation was investigated using a combination of ab initio electronic structure theory, ME calculations, and premixed flame simulations using a new HNNO kinetic sub-model. While (for simplicity) HNNO is used throughout the paper to collectively denote trans-HNNO, cis-HNNO, and ONHN, the theoretical calculations and kinetic modeling treat each isomer separately (similar to previous theoretical studies [13,23]). For example, the two main HNNO species, trans-HNNO and cis-HNNO (which is higher in energy by 5.9 kcal/mol) are separated by a torsional barrier ~23 kcal/mol above trans-HNNO, which is large enough to make trans- and cis-structures of HNNO chemically distinguishable.

2.1. Theoretical kinetics calculations

2.1.1. H + N_2O

Pressure-dependent rate constants for H + N_2O were obtained via ME calculations using a previously published PES from [13] (shown in Fig. 1), which did not report pressure-dependent rate constants for HNNO stabilization. The calculations were performed using the Variflex code [25]. Phenomenological rate coefficients were calculated for temperatures ranging from 300 K to 2500 K and pressures ranging from 0.001 atm to 1000 atm.

2.1.2. HNNO + O_2

The PES and pressure-dependent rate constants were obtained via ab initio electronic structure theory and RRKM/ME calculations. Optimized geometries, vibrational frequencies, and zero-point energy corrections for all the stationary points on the PES were calculated using density functional theory (DFT) employing the ωB97X-D method [26] with the aug-cc-pVTZ basis set as implemented in Gaussian 16 [27]. The proper reactants and products of each transition state were confirmed via intrinsic reaction coordinate (IRC) analysis. High-level single-point energies for all stationary points were obtained through extrapolations of CCSD(T)/aug-cc-pVTZ and CCSD(T)/aug-cc-pVQZ energies to the complete basis set (CBS) as implemented in Molpro [28].

Pressure-dependent rate coefficients were obtained via RRKM/ME calculations using the

MESS code [29]. The internal degrees of freedom for all stationary points are treated via rigid rotor harmonic oscillator (RRHO) assumptions except for the low-frequency torsional modes, which are treated as hindered rotors with hindrance potentials obtained via relaxed energy scans at the ωB97X-D/aug-cc-pVTZ level of theory. Tunneling corrections were made using the asymmetric Eckart model. The collisional energy transfer function was approximated by a single-exponential-down model with $\Delta E_{down} = 100(T/298)^{0.85}$ cm^{-1} and Lennard-Jones model with σ = 3.47 Å and ϵ = 79.2 cm^{-1} for Ar as the bath gas. Phenomenological rate coefficients were calculated for temperatures ranging from 500 K to 2500 K and pressures ranging from 0.01 atm to 1000 atm.

2.2. Kinetic modeling

A kinetic sub-model (Table 1) was constructed to describe pressure-dependent HNNO formation from H + N_2O and its consumption via reaction with common reactive partners: O_2, OH, H, and O. The model includes a number of rate constant expressions derived from ab initio theoretical kinetics calculations: pressure-dependent fits to ME calculations on the H + N_2O PES from [13] (including pressure-dependent HNNO formation); pressure-dependent fits to ME calculations for OH addition to the N adjacent to O in HNNO using the PES from [23]; and Arrhenius fits to ME calculations using the present PES for HNNO + O_2 (whose rate constants we find to have minimal pressure dependence). The vast majority of reactions on the H + N_2O PES and the PES corresponding to OH addition to the N adjacent to O in HNNO were treated using PLOG fits. However, as described in our previous work [30,31], present combustion codes are either unable to accommodate collider-specific rate constants for reactions in PLOG format or implement the classic linear mixture rule (both of which are problematic [30,32–34]).

Recognizing the importance of using even estimated third-body efficiencies for key reactions in flame simulations [35] (where large amounts of H_2O is present in the burned gas region and reaction zone [36]), the rate constants for the three most important pressure-dependent HNNO reactions were instead expressed in Troe format along with typical third-body efficiencies for common bath gases (with the values used for H + O_2 (+M) in [37] which are also consistent with recent studies [34,38,39]). As a cautionary note, these Troe expressions were derived from fits (and therefore only provide a valid representation) of rate constants over the pressure range of 0.001 to 1000 atm and are not meant to correspond to actual low or high-pressure limits. The rationale for representing these three most important pressure-dependent reactions in Troe format is that it allows specification of typical third-body efficiencies and is implemented in combustion codes in a way that is more similar to our reduced-pressure linear mixture rule [30,32] (which captures mixture effects much more accurately than the linear mixture rule [30,32–34]).

This treatment is then augmented by additional reactions that reflect other possible consumption routes for HNNO with rate constants and products based on our preliminary ab initio calculations. These calculations suggest that H, OH, and O add to HNNO with no intrinsic energy barrier to form H_2NNO^*, $H_2NNO_2^*$, and $HNNO_2^*$ complexes that can dissociate via numerous submerged channels to various products. For example, our calculations suggest that H_2NNO^* resulting from H + HNNO can dissociate to NH_2 + NO, H_2O + N_2, and N_2 + H + OH (consistent with [21,22]); they suggest that $H_2NNO_2^*$ resulting from OH + HNNO (at the N site adjacent to H in HNNO) can dissociate to HNOH + NO and H_2O + N_2O (consistent with [24]); and $HNNO_2^*$ resulting from O + HNNO can dissociate to HNO + NO and OH + N_2O. The rate constants for H + HNNO in the sub-model listed in Table 1 are based on our tentative theoretical calculations near 1000 K and the rate constants for OH + HNNO (at sites other than the N adjacent to O) and O + HNNO are simply estimated with values close to the collision limit and the anticipated products indicated above.

This HNNO sub-model (or a portion thereof) was then added to the recent nitrogen kinetics model from Glarborg et al. [2] to create four different modified versions: one that only replaces the treatment of reactions on the H + N_2O PES with our present pressure-dependent fits for all reactions except those involving HNNO (labeled 'w/o HNNO'); one that additionally includes the pressure-dependent fits for HNNO formation and unimolecular reactions and Arrhenius fits for HNNO + O_2 (labeled 'w/ HNNO, w/ HNNO + O_2'); one that additionally includes the abovementioned HNNO + radical reactions with ab initio calculated and/or estimated rate constants (labeled 'w/ HNNO, w/ HNNO + O_2, w/ HNNO + radicals'); and one that uses 5 times higher values for the estimated rate constants (to assess the impact of uncertainties in the estimates; labeled 'w/ HNNO, w/ HNNO + O_2, w/ 5 x HNNO + radicals'). NO predictions in freely propagating flames using these four models were then performed using the Cantera code and compared to ascertain the role of HNNO in NO_x formation via the pathways discussed.

3. Results and discussion

3.1. $H + N_2O$

Pressure-dependent rate constants for H + N_2O to the three main product channels (stabilized HNNO, N_2 + OH, and NH + NO) from the ME

Table 1
Selected reactions from the HNNO sub-model.

			A	n	E_a
(1)	H + N_2O (+M) → t-ONNH (+M) [a]	k_∞	1.70E+04	3.05	6.53E+03
		k_0	1.27E+27	-3.48	7.03E+03
		$F_c = 0.12$			
		$\varepsilon_{H_2} = 3.0$, $\varepsilon_{H_2O} = 21.0$, $\varepsilon_{O_2} = 1.1$, $\varepsilon_{N_2} = 1.5$			
(2)	H + N_2O (+M) → c-ONNH (+M) [a]	k_∞	2.37E-02	4.81	4.79E+03
		k_0	1.23E+25	-2.94	6.77E+03
		$F_c = 0.10$			
		$\varepsilon_{H_2} = 3.0$, $\varepsilon_{H_2O} = 21.0$, $\varepsilon_{O_2} = 1.1$, $\varepsilon_{N_2} = 1.5$			
(3)	t-ONNH (+M) → c-ONNH (+M) [a]	k_∞	1.34E+04	3.36	2.30E+04
		k_0	1.03E+17	-0.80	1.69E+04
		$F_c = 0.075$			
		$\varepsilon_{H_2} = 3.0$, $\varepsilon_{H_2O} = 21.0$, $\varepsilon_{O_2} = 1.1$, $\varepsilon_{N_2} = 1.5$			
(4)	O_2 + t-ONNH → HO_2 + N_2O [a]		3.66E-02	4.34	1.20E+04
(5)	O_2 + t-ONNH → NO + HNO_2 [a]		2.87E+03	2.44	3.10E+04
(6)	O_2 + t-ONNH → O_2 + c-ONNH [a]		1.05E+04	2.09	3.72E+04
(7)	O_2 + c-ONNH → HO_2 + N_2O [a]		9.87E+00	3.50	1.48E+04
(8)	O_2 + c-ONNH → NO + HNO_2 [a]		5.84E+04	2.19	3.12E+04
(9)	OH + t-ONNH → HNOH + NO [c]		3.00E+13	0.00	0.00
(10)	OH + t-ONNH → H_2O + N_2O [a,b]	Duplicate	9.17E+13	-0.55	3.38E+02
		Duplicate	3.00E+13	0.00	0.00
(11)	OH + t-ONNH → NH_2 + NO_2 [a,b]		2.24E+16,	-1.44	1.23E+03
(12)	OH + c-ONNH → HNOH + NO [c]		3.00E+13	0.00	0.00
(13)	OH + c-ONNH → H_2O + N_2O [a,b]	Duplicate	5.96E+14	-0.91	6.68E+02
		Duplicate	3.00E+13	0.00	0.00
(14)	OH + c-ONNH → NH_2 + NO_2 [a,b]		1.50E+14	-0.65	6.26E+02
(15)	OH + c-ONNH → OH + t-ONNH [a,b]		8.21E+12	-0.30	1.16E+03
(16)	H + t-ONNH → NH_2 + NO [c]		4.00E+13	0.00	0.00
(17)	H + t-ONNH → H + N_2 + OH [c]		1.50E+13	0.00	0.00
(18)	H + t-ONNH → H_2O + N_2 [c]		6.00E+12	0.00	0.00
(19)	H + c-ONNH → H + t-ONNH [c]		1.00E+13	0.00	0.00
(20)	H + c-ONNH → NH_2 + N [c]		1.80E+13	0.00	0.00
(21)	H + c-ONNH → H + N_2 + OH [c]		6.00E+11	0.00	0.00
(22)	H + c-ONNH → H_2O + N_2 [c]		9.00E+11	0.00	0.00
(23)	O + t-ONNH → HNO + NO [c]		6.00E+13	0.00	0.00
(24)	O + t-ONNH → OH + N_2O [c]		6.00E+13	0.00	0.00
(25)	O + c-ONNH → HNO + NO [c]		6.00E+13	0.00	0.00
(26)	O + c-ONNH → OH + N_2O [c]		6.00E+13	0.00	0.00

* Units are cm^3, mol, s, cal, K; $k = AT^n \exp(-E_a/RT)$.
[a] Calculated from RRKM/ME simulations.
[b] Pressure = 0.001 atm
[c] Estimated based on preliminary ab initio calculations.

calculations are shown in Fig. 2. Over the relevant temperature and pressure range, the rate constants for the bimolecular product channels show no noticeable pressure dependence. On the other hand, the rate constants for HNNO stabilization increase considerably with pressure – with stabilized HNNO being the dominant product at lower temperatures and higher pressures. Above 10 atm, HNNO is the major product up to ~1100 K and is dominant over NH + NO up to ~1500 K.

The strong pressure dependence for HNNO stabilization from N_2O + H and lack of pressure dependence for the bimolecular products from N_2O + H can be attributed to the fact that HNNO* complexes with sufficient energy to form bimolecular products have faster dissociation rates in general (including back dissociation to N_2O + H). Consequently, collisions are not important for the higher energy states responsible for bimolecular products but are important for the lower energy states responsible for HNNO stabilization.

While the amount of stabilized HNNO increases with pressure, the branching ratio among HNNO isomers is largely independent of pressure, where trans-HNNO and cis-HNNO are formed in comparable amounts from H + N_2O with trans-HNNO comprising ~70% of stabilized HNNO below 1000 K and ~50% of stabilized HNNO at 2000 K at essentially all relevant pressures. ONHN comprises less than 0.1% at temperatures below 1100 K and less than 1% at temperatures below 2000 K.

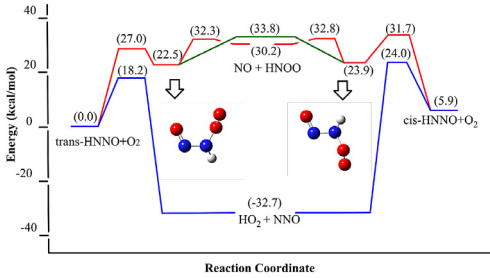

Fig. 3. Potential energy surface (PES) consisting of addition and abstraction reation pathways from trans-HNNO + O_2 and cis-HNNO + O_2 constructed at CCSD(T)/CBS//ωB97X-D/aug-cc-pVTZ level of theory.

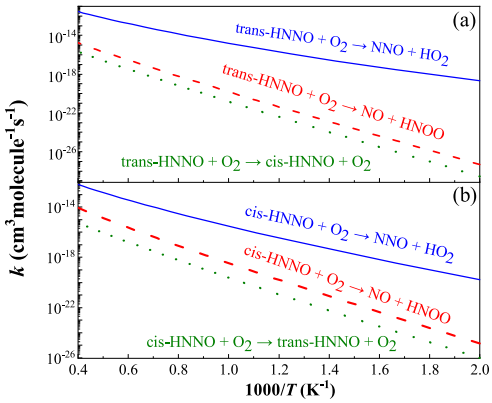

Fig. 4. Predicted rate constants at pressure of 10.0 atm between the main reaction channels from (a) trans-HNNO + O_2 and (b) cis-HNNO + O_2, respectively.

3.2. *HNNO + O_2*

3.2.1. *Potential Energy Surface*

The PES consisting of the energetically favorable channels for the HNNO + O_2 reaction was constructed at the CCSD(T)/CBS[aug-cc-pVQZ:aug-cc-pVTZ]//ωB97X-D/aug-cc-pVTZ level of theory. Fig. 3 shows a simplified version of the PES which includes only the kinetically relevant channels at the relevant temperatures and pressures. All energies are expressed relative to the sum of the energy of trans-HNNO and O_2, which was chosen as a reference and set as zero. Despite their different structure, trans-HNNO and cis-HNNO are found to exhibit similar reactivity with O_2 – albeit through transition states having distinct first-order saddle points. Based on the T1 diagnostics for some stationary points being somewhat higher than usual thresholds for single-reference calculations (e.g. 0.031 for t-HNNO and 0.045 for trans-HNNO + O_2 → NNO + HO_2, cf. Table S1 in the Supplemental Material), multi-reference effects may introduce somewhat higher-than-typical uncertainties in the coupled-cluster calculations but are not expected to impact the present conclusions regarding the main products from HNNO + O_2 or the role of HNNO + O_2 relative to HNNO + radical reactions.

In general, there are two active sites of HNNO for O_2 attack, one of which is the H atom and the other one is the N atom connected to the H atom. Attack on the H atom results in direct H abstraction to yield HO_2 + NNO via distinct saddle points for trans-HNNO and cis-HNNO. The barriers for H abstraction by O_2 for both trans-HNNO and cis-HNNO are found to be ~18 kcal/mol above each of the reactants, respectively (such that the relative energy for abstraction by O_2 for cis-HNNO, whose relative energy is 5.9 kcal/mol higher than trans-HNNO, is 24.0 kcal/mol above trans-HNNO + O_2).

Attack on the active N site results in O_2 addition to yield HN(OO)NO radicals (with geometries as shown in Fig. 3) via distinct first-order saddle points for both trans-HNNO and cis-HNNO. Both addition channels are endothermic. For O_2 addition to trans-HNNO, the transition state has a relative energy of 27.0 kcal/mol to form anti-HN(OO)NO with relative energy of 22.5 kcal/mol above trans-HNNO + O_2. For O_2 addition to cis-HNNO, the transition state has a relative energy of 31.7 kcal/mol (25.8 kcal/mol) to form syn-HN(OO)NO with relative energy of 23.9 kcal/mol (18.0 kcal/mol) above trans-HNNO + O_2 (cis-HNNO + O_2).

Both syn- and anti-HN(OO)NO radicals can also dissociate to NO and HNO_2 by breaking the N–N bond with a barrier of ~32 kcal/mol above trans-HNNO + O_2, interconvert through a torsional barrier of 33.2 kcal/mol above trans-HNNO + O_2, or isomerize to other complexes (not shown) to yield other products (not shown) with significantly higher barriers (above 50 kcal/mol relative to trans-HNNO + O_2). ME calculations that include all of these possibilities indicate that the only kinetically relevant channels resulting from addition are the dissociation to NO + HNO_2 and interconversion and, for simplicity, the pathways proceedings via these other isomers are therefore not shown in Fig. 3.

3.2.2. *Rate Constants*

Rate constants for HNNO + O_2 to the three main product channels (HO_2 + N_2O, NO + HNO_2, and HNNO + O_2) from the ME calculations are shown in Fig. 4. Over the relevant temperature and pressure range, the rate constants for these main product channels show no noticeable pressure dependence. There is no significant stabilization of the HN(OO)NO radicals (or other isomers), whose potential energy wells are not very deep, and, in fact, are not even phenomenologically well-defined chemical species (i.e. the chemically signifi-

cant eigenmodes are merged with the internal energy relaxation eigenmodes [40]) for combustion-relevant temperatures and pressures. Unsurprisingly, given that the abstraction channel has the lowest barrier, abstraction by O_2 to form HO_2 + N_2O has the largest rate constant at all temperatures reaching $\sim 10^{-15}$ cm^3 molec^{-1} s^{-1} at 1000 K and $\sim 10^{-12}$ cm^3 molec^{-1} s^{-1} at 2500 K for both trans-HNNO + O_2 and cis-HNNO + O_2.

The addition-elimination channels, NO + HNO_2 and cis/trans-HNNO + O_2 (which proceeds via a rotational interconversion between anti- and syn-conformers), are orders of magnitude slower. Altogether, the calculated rate constants for each channel indicate that HO_2 + N_2O is the dominant product with NO + HNO_2 having a branching fraction of $\sim 10^{-4}$ (10^{-3}) at 1000 K and $\sim 10^{-3}$ (10^{-2}) at 2500 K for trans-HNNO + O_2 (cis-HNNO + O_2).

3.3. Flame simulations

Model predictions of NO in freely propagating premixed H_2/air flames with equivalence ratio 0.5 at various pressures are shown in Fig. 5 for four models with various treatments of HNNO as described in Section 2.2. Similar to elsewhere [3], the simulated NO is plotted as a function of transformed distance: the "residence time", $\tau = d/s_b$, equal to the distance, d, divided by the burned gas flame speed, s_b.

Overall, the results for the models with and without HNNO formation and HNNO + O_2 show similar NO predictions across the explored conditions – suggesting that HNNO + O_2 does not appear to contribute significantly to NO_x formation at these conditions. However, predictions using the model with HNNO formation, HNNO + O_2, and HNNO + radical reactions differ from those without HNNO chemistry across all pressures. While higher pressures yield higher rate constants for pressure-dependent stabilization reactions responsible for HNNO formation, the simulations also indicate that the considered flames at higher pressures have lower mole fractions of radicals, which are required for more steps of the HNNO mechanism via HNNO + radical reactions than other mechanisms where the N–N bond is broken via reactions involving N_2O or NNH intermediates. Correspondingly, the predictions indicate a complex pressure dependence for the effect of the HNNO mechanism – where the differences between models with and without HNNO + radical reactions are highest at intermediate pressures. Furthermore, predictions with varied rate constants for the HNNO + radical reactions indicate that quantitative predictions of NO are influenced by uncertainties in the estimated rate constants, such that quantitative investigations of the HNNO + radical reactions would be worthwhile.

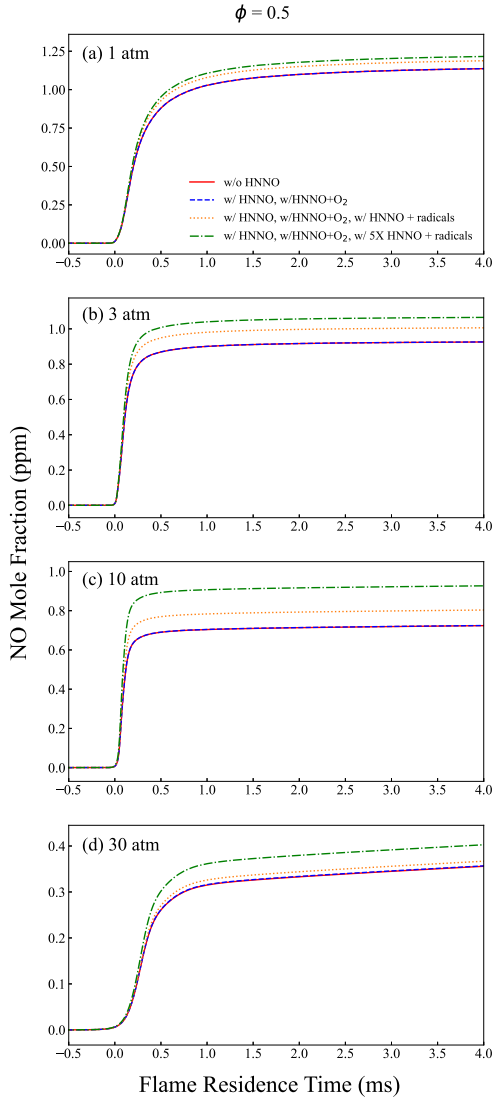

Fig. 5. Predicted NO mole fractions in freely propagating H_2/air flames of equivalence ratio 0.5 vs. flame residence time τ at pressures of (a) 1 atm, (b) 3 atm, (c) 10 atm, and (d) 30 atm

To identify the specific reactions responsible for breaking the N–N bond to facilitate NO_x formation at the present conditions, the rates of each reaction throughout the simulation domain were post-processed to calculate $\omega_k^{\Delta n_N} = \omega_k(n_N{}' - n_N{}'')$ for each reaction, k, where ω_k is the reaction rate of reaction k, n_N' is the maximum number of N atoms in any single species in the reactants, and n_N'' is the maximum number of N atoms in any singles species in the products. In the present H/N/O kinetic models (where all species with more than 1 N atom have an N–N bond and all others do not), non-zero val-

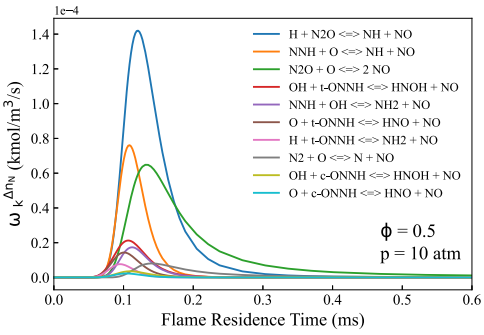

Fig. 6. Ten largest rates of reactions that break an N–N bond calculated using the model with HNNO kinetics in an H_2/air flame of equivalence ratio of 0.5 at 10 atm.

ues for this quantity correspond to the rates of each reaction that results in the N–N bond being broken or formed. These results shown in Fig. 6 indicate that several HNNO + radical reactions (including HNNO + OH, HNNO + O, and HNNO + H) are among the ten highest contributors to N–N bond breaking at 10 atm, where HNNO + OH in particular appears to be the most prominent.

4. Conclusions

The calculated rate constants for the H + N_2O reaction indicate that HNNO is the favored product channel at lower temperatures and higher pressures. In fact, above 10 atm, HNNO is the major product up to ~1100 K and is dominant over NH + NO up to ~1500 K.

Ab initio electronic structure calculations for trans-HNNO (the main HNNO isomer) + O_2 show a barrier for abstraction to HO_2 + N_2O of 18 kcal/mol and a barrier for addition of 27.0 kcal/mol to form an HN(O_2)NO which can decompose to NO + HNO_2 over a barrier of 32.3 kcal/mol; similar reactivity is also found for cis-HNNO + O_2.

The calculated rate constants for the HNNO + O_2 reaction indicate that the dominant reaction product is HO_2 + N_2O with only a minor amount of NO + HNO_2. Both reactions occur with rates that are several orders of magnitude slower than the collision limit and, therefore, are likely sufficiently slow that HNNO + radical reactions are likely competitive (if not dominant) at many flame conditions.

Altogether, our rate constant calculations and kinetic modeling, which also includes calculated/estimated rate constants for HNNO + radical reactions, suggest that HNNO + O_2 mainly recycles HNNO back to N_2O but is sufficiently slow that the primary fate of HNNO in many combustion situations likely involves reactions with radical species, which appear likely to occur quickly and with high NO_x yields. Indeed, flame simulations using this kinetic model suggest that, while HNNO + O_2 may not significantly contribute to NO_x formation (at least for the limited conditions explored here), HNNO + radical reactions may contribute significantly to NO_x formation.

Of course, definitively establishing the role of these HNNO + radical reactions in NO_x would benefit from improved characterization of their rate constants and products in future work. Similarly, while the present study presents an initial step towards understanding the role of HNNO in NO_x formation, establishing a more complete understanding of the role of HNNO would benefit from kinetic modeling studies across a more comprehensive range of conditions.

Declaration of competing interest

The authors declare that they have no known competing financial interests or personal relationships that could have appeared to influence the work reported in this paper.

Acknowledgments

The authors gratefully acknowledge support of this research by the National Science Foundation Combustion and Fire Systems program (CBET-1944004). The authors also thank Stephen Klippenstein for sharing the Variflex files for the N_2O + H and NH_2 + NO_2 reactions.

Supplementary material

Supplementary material associated with this article can be found, in the online version, at doi:10.1016/j.proci.2022.08.044

References

[1] J.A. Miller, C.T. Bowman, Mechanism and modeling of nitrogen chemistry in combustion, Progress in Energy and Combustion Science 15 (4) (1989) 287–338.
[2] P. Glarborg, J.A. Miller, B. Ruscic, S.J. Klippenstein, Modeling nitrogen chemistry in combustion, Progress in Energy and Combustion Science 67 (2018) 31–68.
[3] A. Durocher, G. Bourque, J.M. Bergthorson, Quantifying the Effect of Kinetic Uncertainties on NO Predictions at Engine-Relevant Pressures in Premixed Methane–Air Flames, Journal of Engineering for Gas Turbines and Power 142 (6) (2020). 061008
[4] A.C.A. Lipardi, J.M. Bergthorson, G. Bourque, NOx Emissions Modeling and Uncertainty From Exhaust-Gas-Diluted Flames, Journal of Engineering for Gas Turbines and Power 138 (5) (2015). 051506

[5] Y. Zeldovich, The oxidation of nitrogen in combustion and explosions, Acta Physicochim 21 (1946) 577–628.
[6] C.P. Fenimore, Formation of nitric oxide in premixed hydrocarbon flames, in: Symposium (international) on combustion, volume 13, Elsevier, 1971, pp. 373–380.
[7] L. Moskaleva, M.-C. Lin, The spin-conserved reaction CH+ N_2 → H + NCN: A major pathway to prompt no studied by quantum/statistical theory calculations and kinetic modeling of rate constant, Proceedings of the Combustion Institute 28 (2) (2000) 2393–2401.
[8] J.W. Bozzelli, A.M. Dean, O + NNH: A possible new route for NO_x formation in flames, International Journal of Chemical Kinetics 27 (11) (1995) 1097–1109.
[9] P. Malte, D. Pratt, The role of energy-releasing kinetics in nox formation: fuel-lean, jet-stirred co-air combustion, Combust Sci Tech 9 (5-6) (1974) 221–231.
[10] S.M. Correa, A review of NO_x formation under gas–turbine combustion conditions, Combustion Science and Technology 87 (1-6) (1993) 329–362.
[11] P. Versailles, A. Durocher, G. Bourque, J.M. Bergthorson, Nitric oxide formation in lean, methane-air stagnation flames at supra-atmospheric pressures, Proceedings of the Combustion Institute 37 (2019) 711–718.
[12] S.J. Klippenstein, M. Pfeifle, A.W. Jasper, P. Glarborg, Theory and modeling of relevance to prompt-NO formation at high pressure, Combustion and Flame 195 (2018) 3–17.
[13] S.J. Klippenstein, L.B. Harding, P. Glarborg, J.A. Miller, The role of NNH in NO formation and control, Combustion and Flame 158 (4) (2011) 774–789.
[14] J.W. Bozzelli, A.Y. Chang, A.M. Dean, Analysis of the reactions H + N_2O and NH + NO: Pathways and rate constants over a wide range of temperature and pressure, Symposium (International) on Combustion 25 (1) (1994) 965–974.
[15] N. Lamoureux, H.E. Merhubi, L. Pillier, S. de Persis, P. Desgroux, Modeling of NO formation in low pressure premixed flames, Combustion and Flame 163 (2016) 557–575.
[16] A. Konnov, Implementation of the NCN pathway of prompt-NO formation in the detailed reaction mechanism, Combustion and Flame 156 (2009) 2093–2105.
[17] P. Gokulakrishnan, C.C. Fuller, M.S. Klassen, R.G. Joklik, Y.N. Kochar, S.N. Vaden, T.C. Lieuwen, J.M. Seitzman, Experiments and modeling of propane combustion with vitiation, Combustion and Flame 161 (8) (2014) 2038–2053.
[18] G.P. Smith, D.M. Golden, M. Frenklach, N.W. Moriarty, B. Eiteneer, M. Goldenberg, C.T. Bowman, R.K. Hanson, S. Song, W.C. Gardiner Jr., V. Lissianski, Z. Qin, GRI-Mech3.0.
[19] Sandiegomech, http://combustion.ucsd.edu.
[20] P. Marshall, A. Fontijn, C.F. Melius, High-temperature photochemistry and BAC-MP4 studies of the reaction between ground-state H atoms and N_2O, J Chem Phys 86 (10) (1987) 5540–5549.
[21] J.A. Miller, S.J. Klippenstein, Theoretical considerations in the NH_2 + NO reaction, Journal of Physical Chemistry A 104 (10) (2000) 2061–2069.
[22] D.-C. Fang, L.B. Harding, S.J. Klippenstein, J.A. Miller, A direct transition state theory based analysis of the branching in NH_2 + NO, Faraday discussions 119 (2002) 207–222.
[23] S.J. Klippenstein, L.B. Harding, P. Glarborg, Y. Gao, H. Hu, P. Marshall, Rate constant and branching fraction for the NH_2 + NO_2 reaction, Journal of Physical Chemistry A 117 (37) (2013) 9011–9022.
[24] M.-C. Lin, Y. He, C. Melius, Theoretical interpretation of the kinetics and mechanisms of the HNO + HNO and HNO + 2NO reactions with a unified model, Int Journal Chem Kinet 24 (5) (1992) 489–516.
[25] S. Klippenstein, A. Wagner, R. Dunbar, D. Wardlaw, S. Robertson, J. Miller, Variflex version 2.0, 2008.
[26] J.-D. Chai, M. Head-Gordon, Long-range corrected hybrid density functionals with damped atom–atom dispersion corrections, Physical Chemistry Chemical Physics 10 (44) (2008) 6615–6620.
[27] M. Frisch, G. Trucks, H. Schlegel, G. Scuseria, M. Robb, J. Cheeseman, G. Scalmani, V. Barone, G. Petersson, H. Nakatsuji, et al., Gaussian 16, 2016.
[28] H.-J. Werner, P.J. Knowles, G. Knizia, F.R. Manby, M. Schütz, Molpro: a general-purpose quantum chemistry program package, Computational Molecular Science 2 (2) (2012) 242–253.
[29] Y. Georgievskii, J.A. Miller, M.P. Burke, S.J. Klippenstein, Reformulation and solution of the master equation for multiple-well chemical reactions, Journal of Physical Chemistry A 117 (2013) 12146–12154.
[30] M.P. Burke, R. Song, Evaluating mixture rules for multi-component pressure dependence: H + O_2 (+ M) = HO_2 (+ M), Proceedings of the Combustion Institute 36 (1) (2017) 245–253.
[31] L. Lei, M.P. Burke, Dynamically evaluating mixture effects on multi-channel reactions in flames: A case study for the CH_3 + OH reaction, Proceedings of the Combustion Institute 38 (1) (2021) 433–440.
[32] L. Lei, M.P. Burke, Bath gas mixture effects on multichannel reactions: Insights and representations for systems beyond single-channel reactions, Journal of Physical Chemistry A 123 (3) (2018) 631–649.
[33] L. Lei, M.P. Burke, Evaluating mixture rules and combustion implications for multi-component pressure dependence of allyl + HO_2 reactions, Proceedings of the Combustion Institute 37 (1) (2019) 355–362.
[34] L. Lei, M.P. Burke, Mixture rules and falloff are now major uncertainties in experimentally derived rate parameters for H + O_2 (+ M) → HO_2 (+ M), Combustion and Flame 213 (2020) 467–474.
[35] M.C. Barbet, M.P. Burke, Impact of "missing" third-body efficiencies on kinetic model predictions of combustion properties, Proceedings of the Combustion Institute 38 (1) (2021) 425–432.
[36] M.P. Burke, M. Chaos, F.L. Dryer, Y. Ju, Negative pressure dependence of mass burning rates of H_2/CO/O_2/diluent flames at low flame temperatures, Combustion and Flame 157 (4) (2010) 618–631.
[37] M.P. Burke, M. Chaos, Y. Ju, F.L. Dryer, S.J. Klippenstein, Comprehensive H_2/O_2 kinetic model for high-pressure combustion, International Journal of Chemical Kinetics 44 (7) (2012) 444–474.
[38] R. Choudhary, J.J. Girard, Y. Peng, J. Shao, D.F. Davidson, R.K. Hanson, Measurement of the

reaction rate of H + O_2 + M = HO_2 + M, for M = Ar, N_2, CO_2, at high temperature with a sensitive oh absorption diagnostic, Combustion and Flame 203 (2019) 265–278.

[39] A.W. Jasper, Predicting third-body collision efficiencies for water and other polyatomic baths, Faraday Discuss. (2022), doi:10.1039/D2FD00038E.

[40] J.A. Miller, R. Sivaramakrishnan, Y. Tao, C.F. Goldsmith, M.P. Burke, A.W. Jasper, N. Hansen, N.J. Labbe, P. Glarborg, J. Zádor, Combustion chemistry in the twenty-first century: Developing theory-informed chemical kinetics models, Progress in Energy and Combustion Science 83 (2021) 100886.